Article

Not peer-reviewed version

Depolymerization of PMMA-based Dental Resin Scraps in Dif-ferent Production Scales

Haroldo Jorge da Silva Ribeiro Ribeiro , Armando Costa Ferreira , Caio Campos Ferreira , Lia Martins Pereira , Marcelo Costa Santos , Lauro Henrique Hamoy Guerreiro , Fernanda Paula da Costa Assunção , Sílvio Alex Pereira Da Mota , Douglas Alberto Rocha de Castro , Sergio Duvoisin, Jr. , Luiz Eduardo Pizarro Borges , Nélio Teixeira Machado * , Lucas Pinto Bernar

Posted Date: 16 January 2024

doi: 10.20944/preprints202401.1188.v1

Keywords: PMMA waste; process design; thermogravimetry; differential scanning calorimetry; process scale influence

Article

Depolymerization of PMMA-based Dental Resin Scraps in Different Production Scales

Haroldo Jorge da Silva Ribeiro [1], Armando Costa Ferreira [1], Caio Campos Ferreira [1], Lia Martins Pereira [1], Marcelo Costa Santos [1], Lauro Henrique Hamoy Guerreiro [2], Fernanda Paula da Costa Assunção [2], Sílvio Alex Pereira da Mota [3], Douglas Alberto Rocha de Castro [4], Sergio Duvoisin Jr. [5], Luiz Eduardo Pizarro Borges [6], Nélio Teixeira Machado [1,2,7] * and Lucas Pinto Bernar [1]

[1] Graduate Program of Natural Resources Engineering of Amazon, Campus Profissional-UFPA, Universidade Federal do Pará, Rua Augusto Corrêa N° 1, Belém 66075-110, Brazil
[2] Graduate Program of Civil Engineering, Campus Profissional-UFPA, Universidade Federal do Pará, Rua Augusto Corrêa N° 1, Belém 66075-110, Brazil
[3] Graduate Program of Chemistry, Universidade Federal do Sul e Sudeste do Pará, Folha 31, Quadra 7, Lote Espe-cial - Nova Marabá, CEP: 68.507.590, Marabá/PA, Brasil
[4] Centro Universitário Luterano de Manaus – CEULM/ULBRA, Avenida Carlos Drummond de Andrade N°. 1460, Manaus 69077-730, Brazil
[5] Faculty of Chemical Engineering, Universidade do Estado do Amazonas-UEA, Avenida Darcy Vargas N°. 1200, Manaus 69050-020, Brazil
[6] Laboratory of Catalyst Preparation and Catalytic Cracking, Section of Chemical Engineering, Instituto Militar de Engenharia-IME, Praça General Tibúrcio N°. 80, Rio de Janeiro 22290-270, Brazil
[7] Faculty of Sanitary and Environmental Engineering, Campus Profissional-UFPA, Universidade Federal do Pará, Rua Corrêa N° 1, Belém 66075-900, Brazil
* Correspondence: machado@ufpa.br; Tel.: +55-91-984-620-325

Abstract: This research explores the depolymerization of waste polymethyl methacrylate (PMMAW) from dental material in fixed-bed semi-batch reactors, focusing on three production scales: laboratory, technical, and pilot. The study investigates the thermal degradation mechanism and kinetics of PMMAW through thermogravimetric (TG) and differential scanning calorimetry (DSC) analyses, revealing a two-step degradation process. The heat flow during PMMAW decomposition is measured by DSC, providing essential parameters for designing pyrolysis processes. The results demonstrate the potential of DSC for energetic analysis and process design, with attention to standardization challenges. Material balance analysis across the production scales reveals a temperature gradient across the fixed bed negatively impacting liquid yield and methyl methacrylate (MMA) concentration. Reactor load and power load variables are introduced, demonstrating decreased temperature with increased process scale. The study identifies the influence of temperature on MMA concentration in the liquid fraction, emphasizing the importance of controlling temperature for efficient depolymerization. Furthermore, the research highlights the formation of aromatic hydrocarbons from the remaining char, indicating a shift in liquid composition during the depolymerization process. The study concludes that lower temperatures below 450 °C favor liquid fractions rich in MMA, suggesting the benefits of lower temperatures and slower heating rates in semi-batch depolymerization. The findings contribute to a novel approach in analyzing pyrolysis processes, emphasizing reactor design and economic considerations for recycling viability. Future research aims to refine and standardize the analysis and design protocols for pyrolysis and similar processes.

Keywords: PMMA waste; process design; thermogravimetry; differential scanning calorimetry; process scale influence

1. Introduction

The development and use of synthetic polymers for varied applications led to an increasing generation of plastic waste and environment pollution [1]. Plastic use goes beyond availability and cost, since developed polymers excel in some applications, such as in the case of poly-methyl

 doi:10.20944/preprints202401.1188.v1

methacrylate (PMMA), an important polymer for transplants and prosthetics, especially in ophthalmology and dentistry fields, because of its biocompatibility, transparency, mechanical stability, aesthetic properties, absence of taste and teeth adesion [2–5]. Since PMMA is non-degradable, it is necessary to devise and apply an effective way to recycle this material (and other types of plastic) in order to avoid its accumulation on the environment, polluting terrestrial and marine ecosystems [6,7]. Plastic waste can be recycled through different strategies such as primary (reutilization of the almost unaltered waste for other applications), secondary (mechanical processes such as pelletizing, extrusion, injection molding, drawing and shredding), tertiary (chemical and thermochemical processes such as enzyme treatments, pyrolysis and gasification) and quaternary recycling (incineration). Of these strategies, one of the most promising for recycling of PMMA is the pyrolysis process because research has shown that it is possible to obtain almost complete depolymerization of the PMMA chain, converting it to methyl methacrylate (MMA), its monomer of origin [1].

Primary and secondary recycling of PMMA waste is not advisable due to its use in medical field for implants and undesired properties for mechanical recycling such as thermal stability and hardness [2]. Incineration reduces waste volume by combustion, recovering energy for other applications in the form of steam, displaying high investment and operational costs, as well as higher generation of pollutant gases such as CO_2 [1]. Pyrolysis involves heating the material in absence of oxygen, causing it to thermally decompose in smaller, more volatile molecules generating gaseous, liquid (bio-oil) and solid (char and coke) products, normally used in the production of charcoal from lignocellulosic material [8]. In the case of PMMA and polystyrene, bio-oil composition is rich in their respective monomers (with few side-products), that could be purified and repolymerized to create a "closed loop" in the PMMA industry, with reduced waste generation and value aggregation to its recycling chain [9]. From a process perspective, pyrolysis shows specific advantages such as reduced investment, operating costs, product value and simplicity of operation [1].

PMMA pyrolysis has been extensively studied by researchers worldwide [9–54]. From a process design perspective, some works can be highlighted for a better understanding of our study [9,14,20,40,52-53]. One essential question in process design is the difference between scales of production, what could be expected in the scale-up of a process? Kaminsky et. al. [52], studied the scale-up of a mixed plastic pyrolysis plant utilizing a fluidized bed reactor and reported that homogeneous temperature distribution is easier to be achieved in fluidized bed reactors, allowing a consistent product spectrum. They also reported that tire pyrolysis is not sensitive to the size of the input charge. They compared the product composition of polyethylene pyrolysis in a laboratory (100 g/h) and pilot (20 Kg/h) scales and observed higher production of methane, benzene and naphthalene for pilot scale. They also tested tire pyrolysis in pilot and semi-industrial (120 Kg/h) scale fluidized bed reactor. The feed material of the semi-industrial scale was whole tires and it was observed lower production of gaseous C_5< hydrocarbons, while increasing concentration of higher boiling point aromatic compounds. Even though the work supplies a lot of information about the construction and details of the pyrolysis plants, no comparison is draw about the influence of production scale in the yield of products [52].

Kaminsky et. al. [14], studied PMMA pyrolysis in a fluidized bed for pure and aluminum trihydroxyde (ATH) filled PMMA in two scales of production: in a laboratory unit (3 Kg/h) and in a pilot plant (16-34 Kg/h). They concluded that for fluidized bed reactors there is almost no difference in the scaling-up of PMMA depolymerization, obtaining small differences in yields and MMA purity in both processing plants [14]. Table 1 shows filled PMMA bio-oil yields of 94-96% and MMA purities of 87-90% in the laboratory unit and yields of 93% and MMA content of 83% in the pilot unit. For pure samples, it was observed yields of 97-99% and MMA content of 94-98% in lab compared to 98% of bio-oil yield and MMA purity of 97% in the pilot unit. They also reported that heat losses can be minimized in the pilot plant in a more efficient manner than in the laboratory unit [14]. Sasaki et. al. [40], conducted experiments of pure PMMA depolymerization in fluidized bed reactors in pilot (14.4 Kg/h) and industrial (300 Kg/h) scales and confirmed the small differences observed in the work of

Preprints (www.preprints.org) | NOT PEER-REVIEWED | Posted: 16 January 2024 doi:10.20944/preprints202401.1188.v1

Kaminsky et. al. [14], obtaining almost identical yield and MMA purity for both processing plants [40].

Braido et. al. [20], studied waste PMMA from dental scraps in fixed bed reactors in two process scales: in a small borosilicate glass reactor (30 g of feed) and a larger stainlees steel reactor (2L). They observed liquid yields of 90% and MMA content of 92.8% in the small lab unit against 66.3% and 76.4% respectively in the larger stainless-steel unit, confirming that mass and heat transfer are important to the conversion of PMMA into its monomer for fixed bed reactors [20].

Scale-up of PMMA pyrolysis plants is detailed in the work of Ding et. al. [53], and they compared micro-scale (thermogravimetry) with bench-scale pyrolysis of PMMA in a Fire Propagation Apparatus (FPA) in both experimental and simulation models. They observed the influence of particle size in the kinetics of PMMA depolymerization, where small particle size minimizes the physical mass and heat transfer process, obtaining accurate chemical reactions kinetics. Based on their experimental results, they concluded that it is difficult to scale-up PMMA pyrolysis due to these effects. They also analyzed only the reaction kinetics, not product yield or chemical composition [53].

In a previous study, dos Santos et. al. [9], detailed PMMA pyrolysis process in a semi-batch reactor in pilot scale (reactor volume = 143 L), temperature range of 345-420 °C and it was possible to obtain yields of bio-oil between 48 and 55% (wt.) containing over 90% (area.) of the chromatogram of pure MMA. The material was fed in a relatively large particle size with average vertical and horizontal lengths of 5.94 and 8.69 mm, respectively, and average weight of 100 mg [9]. These results suggest that PMMA depolymerization can be done effectively in semi-batch reactors even with unoptimized mass and heat transfer conditions since these types of reactors are cheaper and easier to operate than a modern fluidized bed or conical spouted reactor [18,52]. Nevertheless, fixed bed reactors suffer from low throughput as the process is done in batch mode, needing high reactor volumes to achieve desired process throughput and to assess the influence of scale-up is maybe more important for these types of reactors. Table 1 summarizes some key aspects of PMMA pyrolysis process detailed in multiple studies, such as PMMA type, temperature, liquid product yield (Y_{LP}), composition of MMA (%MMA), reactor type and process scale.

Table 1. Literature review of PMMA pyrolysis focusing on process scale.

Reference	PMMA type	Temp. (°C)	Y_{LP} (%)	%MMA (.wt%)	Reactor Type	Process Scale
[9]	PMMA waste	345-420	48.2-55.5	83-98	Fixed bed	Pilot (143 L)
[10]	Filled PMMA	450	82.4	57.9	Fluidized bed	Lab (3 Kg/h)
[11]	PMMA waste	490	92.1	91	Fluidized bed	Lab (3 Kg/h)
[12]	PMMA waste	450	98.6	97.2	Fluidized bed	Lab (3 Kg/h)
[14]	Filled and pure PMMA	450-480	94.7-96.2 (filled); 97.5-99.2 (pure)	86.6-90.5 (filled); 93.7-98.4 (pure)	Fluidized bed	Lab (3 Kg/h)
[14]	Filled and pure PMMA	450	92.9 (filled); 98.3 (pure)	83.5 (filled); 96.7 (pure)	Fluidized bed	Pilot (16-34 Kg/h)
[15]	Pure PMMA	450-590	57.3-98.5	95.8-98.7	Fluidized bed	Lab (2g)
[16]	Pure and	440-500	98.1-99.3 (pure);	96.3-97.4 (pure);	Fluidized bed	Lab (1 Kg/h)

Preprints (www.preprints.org) | NOT PEER-REVIEWED | Posted: 16 January 2024 doi:10.20944/preprints202401.1188.v1

	waste PMMA		96.8-98.4 (waste)	95.6-97.3 (waste)		
[17]	Pure and commercial PMMA	450	99.3 (pure); 98.1 (commercial)	99.0 (pure); 96.8 (commercial)	Fixed bed	Lab (1.5 g)
[18]	Commercial PMMA	400-550	90.8-99.1	77.9-86.5	Conical spouted bed	Lab (1.5 g/min)
[20]	Pure and waste PMMA	250-450	9.0-85.0	82.2-99.9	Fixed bed	Lab (30 g)
[20]	Waste PMMA	400	66.3	76.4	Fixed bed	Lab (2L)
[37]	Pure and waste PMMA	450	90-97	90.0-94.8	Fixed bed	Lab (20g)
[38]	Filled PMMA	400-450	18-33	53-80	Fluidized bed	Lab (3 Kg/h)
[40]	Pure PMMA	400	95	95	Fluidized bed	Pilot (14.4 Kg/h)
[40]	Pure PMMA	400	95	94	Fluidized bed	Industrial (300 Kg/h)
[48]	Filled PMMA	300-500	35-97	5-88	Fixed bed	Lab (50 g)

This work aims to evaluate the effect of process scale in the pyrolysis of PMMA dental scrap wastes in fixed bed semi-batch reactors, analyzing the process in a small borosilicate lab unit (30 g), a stainless-steel reactor (2L) and a pilot unit (143 L) observing the effect in the product yields and MMA content in the liquid phase. First, characterization of PMMA dental scrap waste (PMMAW) thermal decomposition is done through thermogravimetry (TG/DTG) and differential scanning calorimetry (DSC). The process is evaluated through measurement of process variables as temperature and reaction time, liquid fraction flow is recorded to observe rate of production and samples were fractioned according to reaction time. Liquid fraction was subjected to laboratory scale fractional distillation in the range of 100-110 °C for further purification. Liquid composition was evaluated by gas chromatography coupled to mass spectrometry (GC-MS) and physical chemical properties as density and viscosity were measured for liquid and distilled samples.

2. Materials and Methods

Figure 1 illustrates the applied methodology used to analyze PMMA depolymerization process in relation to process scale-up.

 doi:10.20944/preprints202401.1188.v1

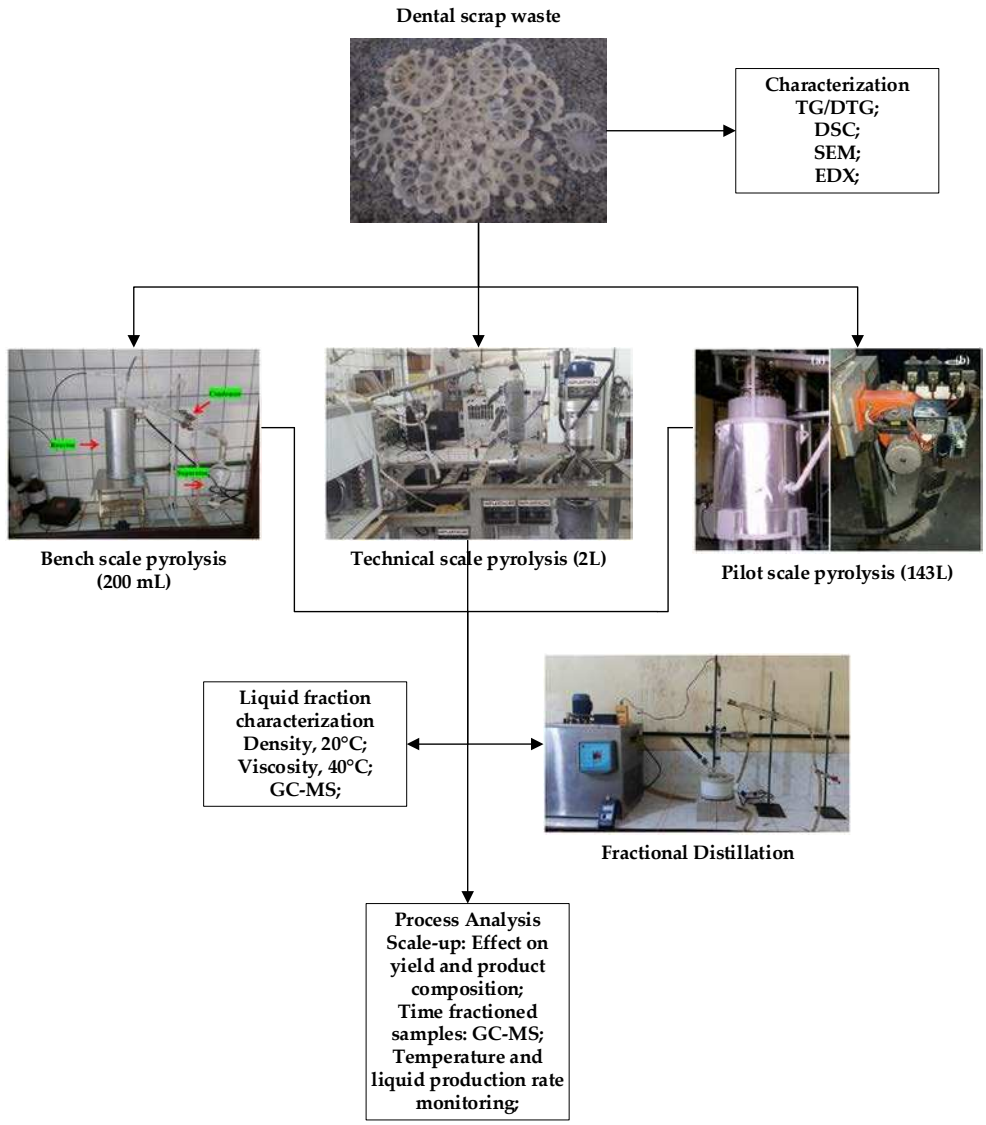

Figure 1. Research methodology applied to analyze process scale-up of PMMA fixed bed depolymerization.

Dental scrap waste (PMMAW) was supplied by Dentsply Indústria e Comércio Ltda (Petropólis, RJ-Brazil) and formulation contains 1.0 .wt% of titanium dioxide (TiO_2) and a crosslinking agent 5.0 .wt% of ethylene dimethacrylate (EGDMA). In order to predict its behavior in pyrolysis, the thermal decomposition of 5 mg of milled PMMAW was analyzed in a Shimadzu thermo analyzer (Kyoto, Japan, Model: DTG 60-H) in a temperature range of 25-600 °C, heat rate of 10 °C/min and nitrogen atmosphere (50 mL/min) in order to check how temperature affects weight loss of the sample. DSC was used to measure the energy flow during thermal decomposition of the sample and it was done in a Netzsch, DSC 404 F1 under nitrogen atmosphere (50 mL/min), temperature range of 25-500 °C and heating rate of 10 °C/min. Scanning electron microscopy (SEM) (FEI company, Hillsboro, OR, USA, Model: Quanta 250 FEG) coupled to chemical analysis detector EDS, using carbon pin stubs specimen, and a high vacuum sputter coater (Leica, Wetzlar, Germany, Model: EM ACE600) was used to check elemental composition of PMMA samples and observation of resin surface.

All three fixed bed pyrolysis plants were accurately described in previous works [9,55–63]. Basically, the three reaction systems are constructed based on a classic semi-batch pyrolysis system (Figure 2) composed by a heated temperature-controlled fixed bed reactor coupled to a tube condenser operating with cooling water. The condensate+gases are separated in another vessel, collecting the liquid fraction and venting the non-condensable gases produced. The lab and technical scale reactors are heated by electrical heaters, of 800 W and 3500 W, respectively. The pilot unit is

Preprints (www.preprints.org) | NOT PEER-REVIEWED | Posted: 16 January 2024 doi:10.20944/preprints202401.1188.v1

heated by an LPG gas burner (0-40 mbar, 5800-34800 W). Since we're focusing on the process scale-up, it is important to mention the dimensions of the three reactors. Table 2 compiles the information about internal diameter (i.d.) and height (h) of the three cylindrical reactors. A typical pyrolysis run uses a ramp of heating rate 10 °C/min until the process temperature of 450 °C. The vapors and liquids formed are collected in the separating drum vessel and temperature recorded each 10 minutes. After the reaction, reactor is cooled naturally and opened to weight the formed char. In the case of technical and pilot scale, samples of liquid fraction were taken at each 10 minutes of reaction in order to evaluate process flow rate and variation of chemical composition with reaction time and process temperature.

Table 2. Dimensions of the three cylindrical reactors used to study the scale-up of PMMA depolymerization.

Reactor	i.d. (mm)	h (mm)	Volume (L)
Borosilicate glass	30	150	0.1
Technical	85	355	2.0
Pilot	300	1800	143

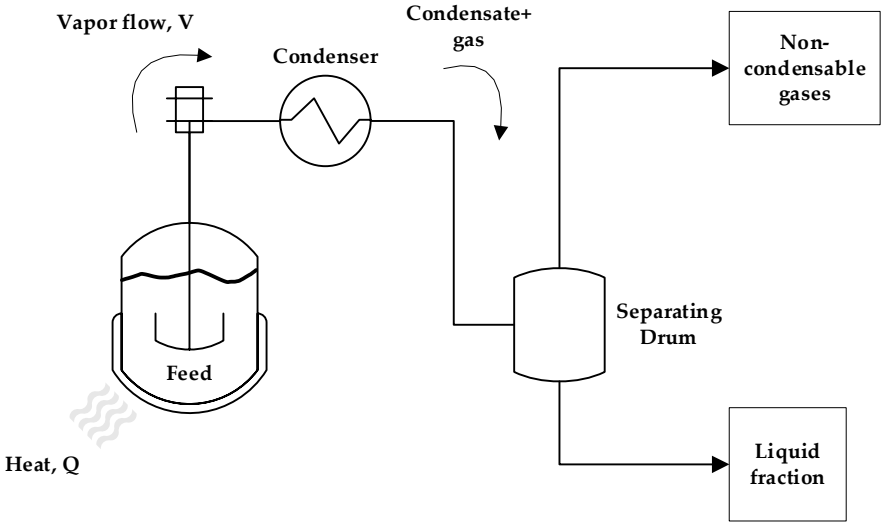

Figure 2. Classical setup of semi-batch fixed bed pyrolysis system.

Liquid fractions of all three reaction systems were subjected to lab-scale (V_{sample}=250 mL) fractional distillation in the boiling range of 100-105 °C in order to obtain purified MMA. Both liquid fraction and distilled product were characterized according to standard procedures of density (ASTM D4052, 25 °C), viscosity (ASTM D445/D446, 40 °C) and refraction index (AOCS Cc 7-25). GC-MS analysis of the samples was done to check chemical composition as described elsewhere [9]. Basically, 1 μL of sample is dissolved in 1 mL of combined solvent acetone:toluene 50/50 v/v and injected in split-mode (1:50) in the GC equipment (Agilent, GC-7890B, MS-5977A), capillary column of fused silica (SLBTM-5ms) (30 m x 0.25 mm x 0.25 mm) and helium as carrier gas. Obtained mass spectra are compared to NIST database and compostion is reported in TIC%.

 doi:10.20944/preprints202401.1188.v1

3. Results

3.1. Thermal Decomposition and Characterization of PMMA Dental Scraps (PMMAW)

PMMAW was characterized by TG/DTG in respect to the weight loss of the sample and DTA and DSC analysis to evaluate the heat flow during the depolymerization process. Thermogravimetry provides useful information when designing pyrolysis or depolymerization processes, for all types of reactor and modes of operation. The small sample size allow uniform distribution of temperature on the feed material and minimize the effects of defficient mass and heat transfer due to particle size, bed thickness and thermal conductivity of the material being analyzed [47]. TG/DTG provide information about the number of stages of decomposition of a sample together with peak temperatures (temperature of maximum decompostion), suggesting the reaction order and kinetics of sample decomposition. The TG/DTG is shown in Figure 3 highlighting the main stage and peak temperature of decomposition of PMMAW. The results show a single decomposition stage beginning at 327 °C and end at 405 °C with peak at 366 °C. The decomposition kinetics of PMMA samples is affected by parameters such as temperature and molecular weight of polymer, changing the thermal decomposition of PMMA polymer and presenting different reaction mechanisms [15]. Barlow et. al. studied PMMA degradation kinetics and mechanisms in the temperature range of 340-460 °C using a micropyrolysis technique (Py-GLC) for PMMA polymers of different molecular weights (MW = 64850-579500 g/mol) and observed that decomposition reaction is a radical depolymerization where the chain backbone of the polymer is split by a radical reaction mechanism and degradation in lower temperatures (340-370 °C) is governed by a reaction mechanism consisting in chain-end initiation followed by depropagation and finally termination by bimolecular interaction. The reaction mechanism scheme is represented by equations (1), (2) and (3), respectively. In this temperature range, the degree of polymerization (represented by the molecular weight) affects negatively the reaction rate, corroborating their proposed mechanism where reaction rate is inversely proportional to the degree of polymerization of the PMMA sample [64].

$$\text{Chain-end Initiation: } P \rightarrow R\cdot + X \quad (1)$$

$$\text{Depropagation: } R\cdot \rightarrow R\cdot + M \quad (2)$$

$$\text{Termination by bimolecular interaction: } R\cdot + R\cdot \rightarrow P[+P] \quad (3)$$

where P is the PMMA polymer, $R\cdot$ is a radical, $X\cdot$ is a small radical which distills out of the system, M is the monomer MMA [64].

Preprints (www.preprints.org) | NOT PEER-REVIEWED | Posted: 16 January 2024 doi:10.20944/preprints202401.1188.v1

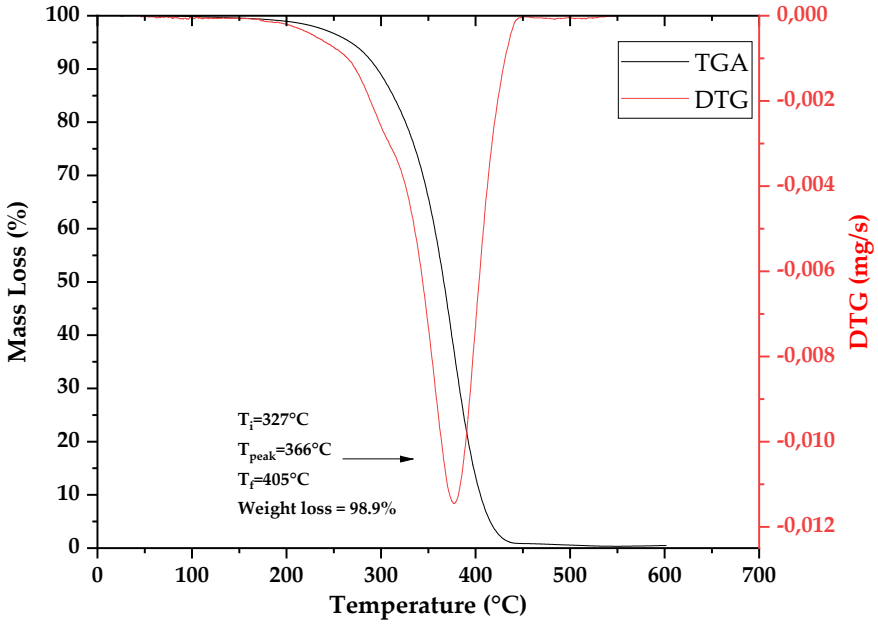

Figure 3. TG/DTG measurement of PMMAW. .

Several authors studied PMMA degradation by TG/DTG and agree that decomposition of some solid PMMA samples can be adequately represented by a single stage in inert atmospheres of nitrogen and argon depending on the molecular weight of the polymer, temperature, type and agents of polymerization [9,13,15,16,18–20,22–24,47]. Peterson et. al. [24], observed that a small first step of decomposition occur at vynilidene end groups but this step is usually overlaped with the following step of degradation by random scission, especially at higher heating rates [24]. In fact, it can be seen in Figure 3 that weight loss starts to occur as early as 200 °C in a slow rate, increasing with temperature until 361 °C. Nevertheless, DTG only shows a single peak of decomposition possibly due to the use of 10 °C/min as heating rate, making it impossible to distinguish between the two peaks of decomposition. Da Ros et. al. [47], proposed a three step degradation mechanism for the thermal decomposition of EGDMA-crosslinked PMMA waste but suggested that a two-step consecutive reaction and single stage decomposition could also represent the more thermally stable sample of crosslinked polymer. Homopolymer PMMA exbihited earlier degradation at 150 °C and more pronounced peaks in the DTG analysis [47]. Manring et. al. [23, 35], suggested that different end-groups may be associated with different thermal behaviour and pointed out that vynil-terminated PMMA degraded at lower temperatures because of the unsaturated end-group, generating a radical unzipping of the polymer chains via chain transfer process and that unsaturated bonds formed by termination in the polymerization process are unstable at the ends of polymer chains. They also commented on the fact about different thermal degradation behaviours depending on the polymerization agent used [23,35]. These observations are also present in the work of Hu et. al. [25], who studied the effects of end-groups in thermal decomposition of PMMA [25].

Hu et. al. [25], conducted several TGA experiments of PMMA samples prepared using different polymerization agents in order to elucidate the thermal degradation mechanism and the called "blocking effect" of different end-groups since the initial temperature of degradation of PMMA seems to be affected by the type of end-group present. The type of end-group depends upon the polymerization agent, so it is possible to increase the thermal stability of the PMMA polymers, degrading only at higher temperatures. They observed that polymerized PMMA initiated with 2,2'-azobisisobutyronitrile (AIBN) presented two stages of weight loss (corroborated by DTG), one of

 doi:10.20944/preprints202401.1188.v1

them at low temperatures between 200-300 °C and the other, more intense, between 320-400 °C. This first peak was not observed for PMMA polymerized using thiols, where the end-group contains specific units as -S-$(CH_2)_{11}$-CH_3, -S-$(CH_2)_2$-COOH and -S-$(CH_2)_2$-OH and thermal degradation occurred only at temperatures higher than 300 °C via main-chain scission, blocking the unzipping via the end unit, particularly at low temperatures [25]. The TGA obtained for PMMAW in this work presented low temperature degradation but not as intense as the ones observed for PMMA-AIBN in the work of Hu et. al. [25], as observed by the single peak in DTG, indicating that the blocking effect can be augmented or supressed by other mechanisms or parameters.

It is worth to note that considerable variability exists in thermal decomposition of PMMA even with rigorous TG procedures and this was pointed by several authors [22,24]. As it was observed earlier, degradation of polymer chain may occur through different mechanisms, influenced by temperature, molecular weight and polymerization agent. Furthermore, thermal degradation of PMMA is usually done in solid-phase and heterogeneous reactions rates are influenced by mass and heat transfer processes. Even though thermogravimetry usually needs low weights (in the order of mg) of ground samples, minimizing mass and heat transfer, some influence is inevitably present, especially in the case of long polymeric chains [9,13,15,16,18–20,22–24,47].

The presence of a crosslinking agent also influences in the mechanism of PMMA degradation. In the case of PMMAW it contains 5.0 .wt% of EGDMA as a crosslinking agent and its effects were studied by Bate&Lehrle [54], and Braido et. al. [20,47]. The study on kinetics of thermal degradation of crosslinked PMMA in a heated filament and analyzed by Py-GC/MS concluded that presence of EGDMA as crosslinking agent exerts a blocking effect in the unzipping of the polymeric chain, showing lower reaction rates when compared to non-crosslinked PMMA even though they initiate by the same mechanism but the unzipping seems to be stabilized when it reaches a crosslinking unit [54]. Indeed, Braido et. al. [20,47], compared homopolymer PMMA and EGDMA-crosslinked PMMA waste thermal degradation by TGA and concluded the homopolymer starts to degrade at lower temperatures, as early as 150 °C, while the crosslinked sample started to degrade at temperatures of 200 °C with a lower rate of mass loss. The PMMAW of this work presented a similar behavior to what is observed for the crosslinked samples of the other authors, showing that crosslinked PMMA is more thermally stable than the pure polymer [20,47,54].

The energetic characterization of the thermal degradation of PMMAW was done by DSC, displayed in Figure 4. Differential scanning calorimetry is a thermal analysis technique where the sample and a reference (normally the empty furnace) are heated on a double-furnace. The heat flow is controlled in a feedback loop in order to maintain equal temperature between the sample and the reference and it is used to compute useful thermodynamic parameters as heat capacity of the sample and the energy traded in physical transformations and chemical reactions [46]. It is commonly used to study material properties as glass transition temperatures, heats of fusion and general calculation of reaction enthalpy [65]. The use of DSC technique to study pyrolysis or gasification processes is not that widespread, mainly because the calculations are done based on the initial weight of the sample and in thermal decomposition processes there is considerable variation of this weight as the feed pyrolyzes into gases. Some authors circumvented this problem considering the mass available at each heat flow peak in simultaneous TG/DSC equipment [66,67]. In order to accurately measure the energy involved in chemical reactions, one must integrate the signal of heat flow x time (peak area) for each detected reaction peak and since there is variation of heat capacity with temperature, the detection of some peaks is not so direct and often, if not always, baseline correction (extraction of heat capacity variation from the curve) is needed to accurately define peaks and integrate its area [67]. Even then, the results have to be closely observed since multiple transformation can be coupled in a single peak, difficulting its analysis.

Preprints (www.preprints.org) | NOT PEER-REVIEWED | Posted: 16 January 2024 doi:10.20944/preprints202401.1188.v1

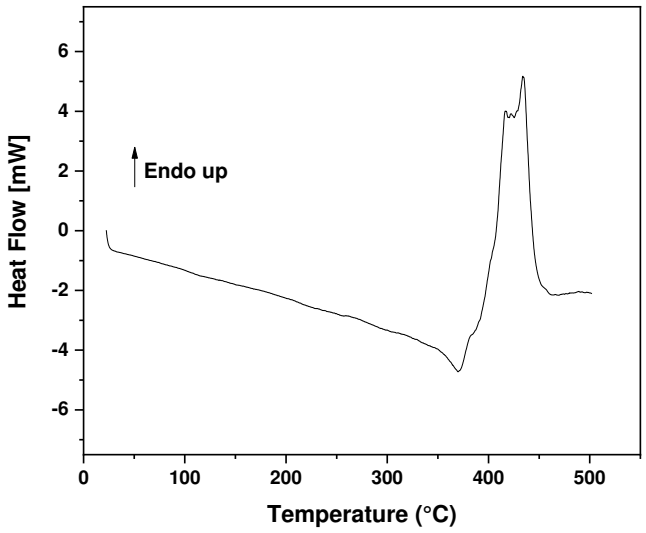

Figure 4. Heat flow measured by DSC of PMMAW at heating rate of 10 °C/min and nitrogen atmosphere.

Varied strategies can be used to extract heat capacity from DSC curve. Chen et. al. [66], determined the heat of biomass (wood) pyrolysis by simultaneous TG/DSC estimating specific heat capacity by a weighted average of heat capacities from the sample and leftover char in the reactor [66]. Other mathematical methods involve graphically fitting functions representing the heat capacity and subtracting them from the DSC curve. A combination of functions can be used when the baseline is sufficiently complex. Figure 5 shows the baseline-corrected DSC curve of PMMAW pyrolysis, done in Origin Software subtracting the baseline using a spline function.

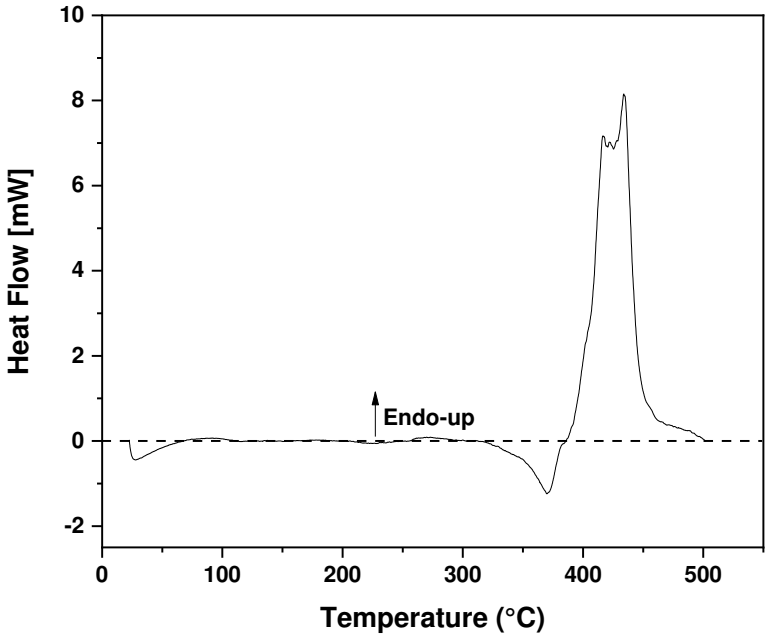

Figure 5. Baseline-corrected (heat capacity extraction) heat flow measurement of PMMAW decomposition.

 doi:10.20944/preprints202401.1188.v1

Analysis of Figure 5 reveals the presence of one large endothermic peak between 370-433 °C. It is difficult to accurately describe energy trades in pyrolysis such as heat of pyrolysis and vaporization enthalpies of products since many processes are coupled and happening at the same time. The actual value of heat of pyrolysis depends heavily on the feedstocks, temperature ranges, heating rate, the extent of secondary reactions and even measurement conditions and accurate determination of this value is challenging. There are incosistent results in literature, ranging from overall endothermic to exothermic [68]. Literature review of DSC applied to PMMA for energetic characterization of its thermal decomposition presents mixed results for its thermal decomposition. Most studies focused on transistions below 200 °C, as glass transition temperatures for composites prepared using PMMA and other plastics [65,69–74] or to check mechanical and thermal properties of the polymer [75–77]. Reports of DSC analysis of PMMA thermal decomposition done under higher temperature conditions are scarce [78–80]. Fiola et. al. [78], analyzed thermal properties of extruded and cast PMMA by DSC finding a endothermic peak between 327 and 427 °C for both samples with values of integrated heat flow (measure of the process enthalpy) of 1.5 J/g [78]. Wang et. al. [80], tested PMMA composites through DSC under nitrogen atmosphere and different heating rates (10-30 °C/min) and found 3 stages of decomposition with 3 endothermic peaks [80]. Alonso et. al. [79], used DSC to analyze the thermal decomposition of PMMA under different mass quantities and different atmospheres, observing endothermic peaks in nitrogen atmosphere [79].

Accurate determination of the energy involved in each transition corresponding to individual peaks can be difficult and by observing Figure 5, one could make the assumption that exists more than one peak in decomposition of PMMAW, including one previous exothermic step and a later third endothermic stage. Analysis by a single step mechanism was an initial assumption based in academic literature [9,13,15,16,18–20,22–24,47] and to keep its description simple and general in order to be applied to other feedstocks, even though it is possible to describe thermal degradation of PMMA in more than one step [20,47]. DSC has quantitative capabilites but they are better applied to well known processes and reactions where knowledge of the actual mechanism involved is modelled in the calculations, including equipment-specific parameters such as neutral baseline (heat flow difference between an empty pan and the reference). Correction of baseline can also be done by using a modelled equation of c_p x T and considering heat capacity of the remaining char [78]. For pyrolysis reactions, the weight of the sample changes as the vapors flow out of the system and a correction is needed for calculation of individual peaks energy [68].

In the thermal decomposition of PMMA, there are some simplifications and complications associated to calculation of related energy of individual DSC peaks. PMMA decomposition stages can be approximated to a single step as seen in DTG of Figure 3 and practically no char is generated, so no correction is needed for the variation of weight of the sample. Since no char is generated, influence of char heat capacity to the DSC curve is minimal. The product of PMMA depolymerization is mainly MMA largely simplifying the analysis of thermodynamic parameters.

The complications arise when considering the processes involved in PMMA thermal decomposition, mainly because of specifics related to the actual structure of the polymer such as the presence of crosslinking agents, end-groups and the degree of polymerization (molecular weight of the polymer), generating a large variation in values of known thermodynamic quantities as the heat of decomposition of the sample and making the DSC energetic analysis model-specific. Nevertheless, integration of the endothermic peak generated values of 423 J/g with integral heat (entire energy used, including heating the sample, frequently called heat of gasification) of 1748 J/g. The peak seems related to the vaporization enthalpy of MMA of 40.1 KJ/mol or 401 J/g but higher quantities were expected since heat of depolymerization of PMMA should be in the range of 560 J/g. Indeed, decomposition heat of PMMA reported are in the range of 820 J/g [78]. The heat of gasification obtained in PMMAW DSC is in accord with others numbers reported for thermal decomposition of PMMA [78–80].

 doi:10.20944/preprints202401.1188.v1

3.2. Process Analysis

3.2.1. Scaling-Up Effect on the Yield of Products

The process conditions and yields of products obtained in the three scales of production are summarized in Table 3. It can be observed that very different liquid yields are achieved when comparing laboratory and the other two scales of production. Liquid yields tend to reduce with increase in volume of the reactor. As it was discussed earlier, in order for PMMA decomposition to occur in a single step of reaction, with small production of side products and produce a consistent liquid composition, it is necessary a higher mass and heat transfer, allowing the reaction to proceed with uniform temperature across all sections of the reactor, condition observed in the case of fluidized bed reactors [14,40]. In the case of unstirred fixed bed reactors loaded with solid feed, such as PMMAW, there is a temperature gradient from the external wall of the tube reactors to their center (bulk temperature). In the case of the small glass reactor, the distance of the wall to the center is only 15 mm and the temperature gradient is small. This can be observed by the difference in the temperature of initial condensation of products in the three reactors: while technical and pilot depolymerization condensed products in temperatures of 109 and 113 °C, respectively, the laboratory experiments displayed initial condensation temperature of 230 °C. This effect can be further amplified or minimized by material type and particle size, since the heat conductivity, particle size and packing of the bed all influence the mass and heat transfer occurring during the depolymerization reaction. The char shape obtained in the experiments was very reminiscent of the original material and DSC analysis (Figure 4) did not show a characteristic change in heat capacity indicating melting of the sample, suggesting that the material remained in its original shape during pyrolysis.

It has been defined two variables to assist in understanding our analysis, Reactor Load (Kg/L) and Power Load (W/Kg). Reactor Load is the ratio of weight of PMMAW to volume of the reactor and it is a measure of the occupation of the fixed bed, while Power Load is defined as the ratio of available heating power to the weight of feed in the reactor. It can be observed that Reactor Load decreased with the scale-up, meaning that for larger volumes (technical and pilot), the feed was occupying a smaller portion of the fixed bed. This should minimize the temperature gradient to the center of the fixed bed, but it can be observed that Power Load still decreases with scale-up and reaction takes more time in technical and Pilot scales. This decrease in power load associated with the larger volume of feed in the three reactors and the low thermal conductivity of the PMMAW bed further increase the temperature gradient to the center of reaction so, while the bulk temperature in technical and pilot scales reached values of 450 °C, it is probable that higher values were achieved near the wall of the reactor, increasing cracking of molecules and gas formation. The Power Load of 20000 W/Kg in the laboratory unit is sufficient to achieve uniform temperature across the fixed bed of feed, making it easier to control the reaction with better temperature control. It is important to mention that Power Load only considers the available power supplied by the equipment, not the actual power used in the experiment. The results showed that lower reactor loads associated with higher power loads increase the amount of gas formed probably due to increase in temperature gradient across the fixed bed radius. Temperature increases in fixed bed pyrolysis have been shown to affect negatively liquid yield and MMA concentration in pyrolysis oil due to side reactions influenced by higher temperatures [9], as shown in Figure 6, displaying the influence of temperature in product yields for technical scale. From 425 to 450 °C, liquid yields decreased from 82 to 61 wt.% indicating that temperature largely influences the yields of products. Unlike in the technical and pilot scales, reactor temperature thermocouple was situated outside of the reactor and possibly reactor actual temperatures were lower while for the technical and pilot scales, thermocouple is situated in the center of fixed bed and temperatures at the edges of the reactors are higher than the setpoint of 450 °C, augmenting the production of side products in liquid and gaseous phases. The slower heating rates in the larger fixed bed of PMMAW also increased char yields with process scale, corroborating what it is observed in academic literature for many types of materials [55–57].

Preprints (www.preprints.org) | NOT PEER-REVIEWED | Posted: 16 January 2024 doi:10.20944/preprints202401.1188.v1

Table 3. Process conditions and yields of reaction products by thermal degradation of PMMA based dental resins fragments/residues at 450 °C, atmospheric pressure, in laboratory, technical and pilot scales.

Process Conditions	Temperature [°C]		
	450		
	Laboratory	Semi-Pilot	Pilot
Mass of feed [g]	40.00	625.00	20000
Reactor Volume [L]	0.1	2.0	143
Reactor load [Kg/L]	0.40	0.31	0.14
Power Load [W/Kg]	20000	5600	290-1740
Reaction time [min]	60	100	130
Temperature of liquid condensation [°C]	230	109	113
Final temperature [°C]	450	455	458
Mass of coke [g]	0.29	15.11	1700
Mass of liquid [g]	38.31	384.70	11836.3
Mass of gas [g]	1.46	223.94	6463.7
Yield of liquid [%]	**95.63**	**61.67**	**59.18**
Yield of coke [%]	**3.64**	**2.43**	**8.50**
Yield of gas [%]	**0.73**	**35.90**	**32.32**

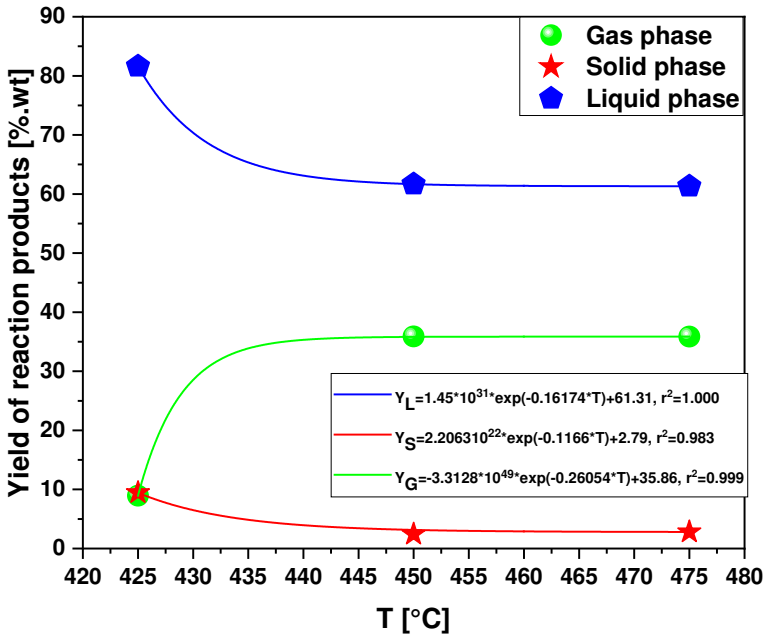

Figure 6. Effect of temperature on the yield of liquid, coke and gas phase products in the depolymerization of PMMA-based dental scraps at 425, 450 and 475 °C in technical scale.

Since pyrolysis process products are influenced by temperature and heating rates, it can be concluded that characteristics of the feed as specific heat, thermal conductivity and particle size and characteristics of the process such as reactor geometry, heating mode and residence time are connected to temperature effects, influencing the yields of products. This is especially true for fixed bed reactors, where large vessels tend to show far more temperature differences across the fixed bed geometry packed inside the reactor. As it will be seen in Section 3.2.2, it seems that temperatures

Preprints (www.preprints.org) | NOT PEER-REVIEWED | Posted: 16 January 2024 doi:10.20944/preprints202401.1188.v1

below 425 °C tend to produce highest amount of liquid phase presenting also highest content of MMA, at least for fixed bed semi-batch reactors.

In semi-batch pyrolysis, where vapors flow continually out of the heated reaction zone by cracking and vaporization (endothermic processes), reaction temperature tends to stay in specific ranges determined by reaction kinetics and present substances, consuming the heat supplied by the electrical heater to conduct physical or chemical transformations. For larger reactors, almost no difference is observed in the reactor thermocouple until the endothermic processes complete, in this case the depolymerization reaction of PMMAW and subsequent vaporization of products. As its thermal decomposition occurs around 150-200 °C and main product from depolymerization of PMMAW is MMA, with a boiling point of 101 °C, reactors temperature tends to remain in the 200 °C range for larger vessels. This can be seen in the graph of Figure 7, displaying the reactor temperature profile of the pilot reactor and recovered liquid phase percentual related to the total liquid phase obtained. More than 93 wt.% of the liquid phase collected was produced between 145 and 208 °C. Only a small percentage of the liquid phase was collected in higher temperatures. It can be observed that the vapor flow production halted the reactor heating producing an inflection at 40 minutes of reaction time and reactor temperature changed little. After almost all liquid had vaporized, temperature started rising again to the desired setpoint. Nevertheless, different process temperatures of PMMAW depolymerization (425-475 °C) was tested in the technical plant and considerable differences were observed. First, liquid yields were far higher for 425 °C, reaching values of 81.6%, where for 450 and 475 °C, 61% (Figure 6). As it will be seen in Section 3.2.2, MMA concentration also varied with temperature, reducing with increasing temperature, revealing that even though it is not possible to choose a desired reaction temperature (defined by process thermodynamics), it is possible to obtain different heating rates that largely influences products yields and quality.

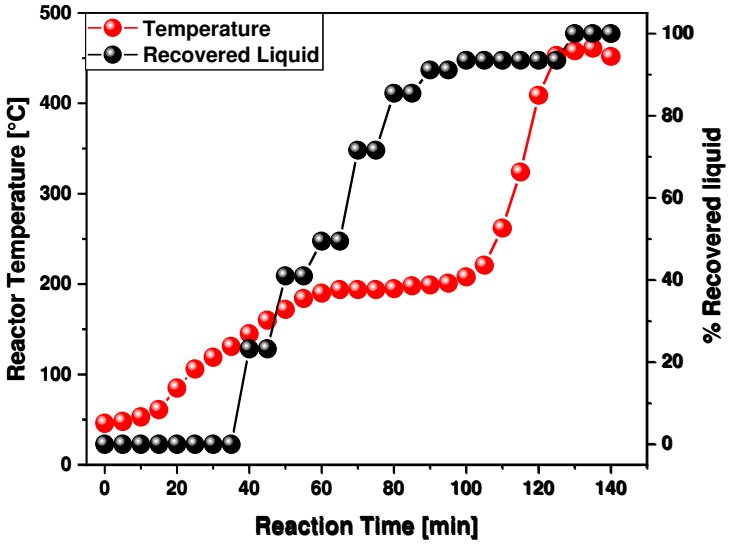

Figure 7. Pilot reactor temperature and % recovered liquid phase profile of PMMAW depolymerization at 450 °C.

It is interesting to note that this temperature behavior is only present for the larger vessels: the technical and pilot plants. For the laboratory scale, where the thermocouple is positioned outside of the reactor and there is considerable power load (20000 W/Kg), meaning that temperature gradients across the geometry of the fixed bed are low. Figure 8 compares the temperature profile of the three production scales and shows that pyrolysis took place between 193-369 °C, similar to what is presented in TG analysis (Figure 3). The adjustment and control of temperature in semi-batch reactors is related to the amount of power supplied and the quantity of feed in the reactor. For low power loads, where it is not possible to adjust reactor temperature beyond a certain point, process

Preprints (www.preprints.org) | NOT PEER-REVIEWED | Posted: 16 January 2024 doi:10.20944/preprints202401.1188.v1

temperature represents the extent of reaction and the heating rate applied. For higher power loads, it is possible to improve the reaction temperature and for PMMAW, it means a higher yield of liquid phase associated with higher concentration of MMA due to minimization of temperature gradients across the fixed bed.

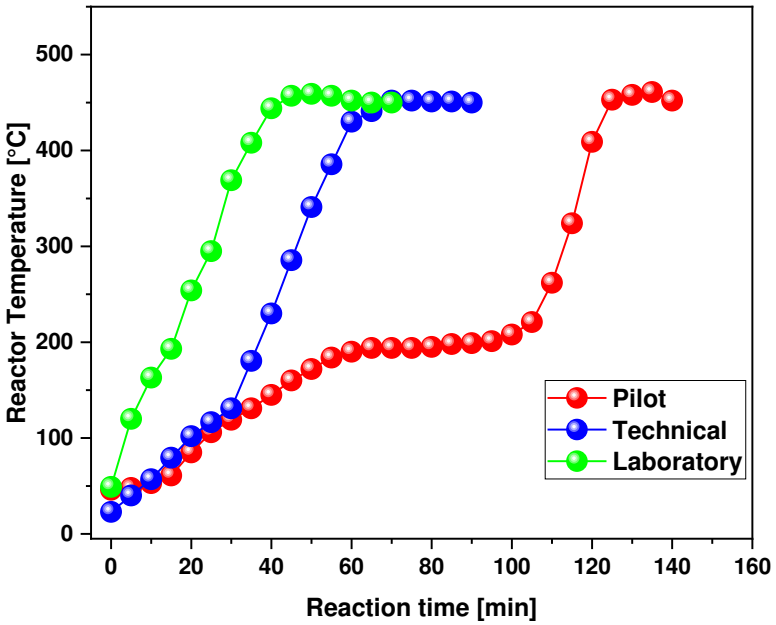

Figure 8. Temperature profile (T x t) of PMMAW depolymerization process in laboratory, technical, and pilot process scales.

Temperature profile of the larger vessels is similar until 50% of the recovered liquid is collected, corresponding to 40 minutes of reaction time. As it is shown in Figure 9, PMMAW depolymerization in technical scale occurred between 102-430 °C, with more than 50% of the recovered liquid being collected before temperatures of 250 °C were reached. From that point, the power load of the technical plant allowed a linear increase of temperature, while collecting more liquid. As it will be seen in Section 3.2.2, it is clear that liquid phase was 100% MMA until 40 minutes of reaction time and afterwards slowly changes to other compounds such as methyl isobutyrate and aromatic hydrocarbons (benzene, toluene, xylene and others). This suggests that for lower power loads, in order to maximize MMA concentration, it is needed lower temperatures, minimizing the formation of side products. Lower power loads mean effective lower heating rates for parts of the PMMAW fixed bed, allowing the formation of more char and stopping the unzipping of the polymeric chain, reducing the formation of MMA. In fact, in the technical and pilot scales, where the formation of char is significative (higher than 5%), the chemical composition of vapors and liquid fraction changes from MMA to chemical compounds normally encountered in the pyrolysis of coal, such as aromatic hydrocarbons [81]. For the laboratory scale, with a high-power load, almost all the material reaches the same temperature, and the reaction is allowed to occur in a few minutes (20 minutes), the formation of char is minimized, and liquid fraction collected is almost exclusively formed by MMA.

Preprints (www.preprints.org) | NOT PEER-REVIEWED | Posted: 16 January 2024 doi:10.20944/preprints202401.1188.v1

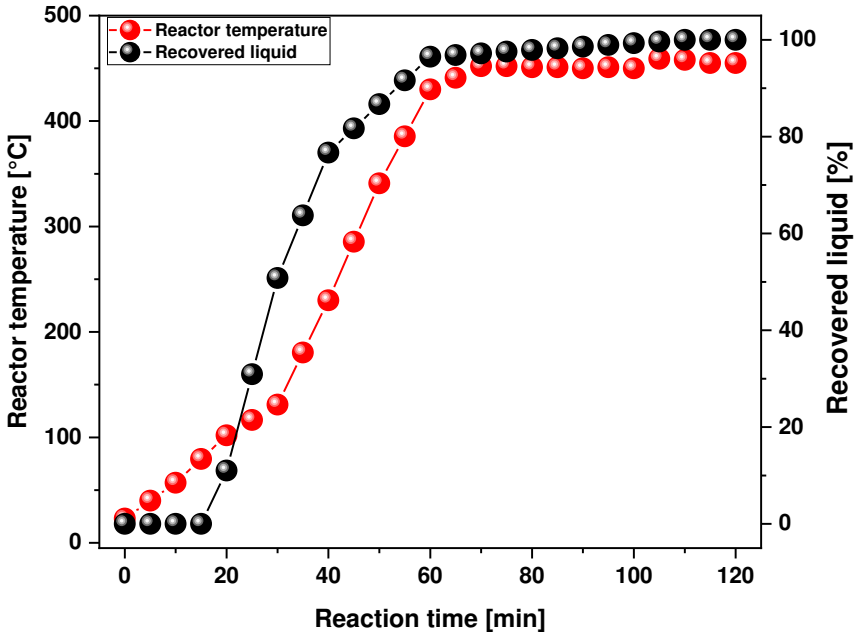

Figure 9. Technical scale reactor temperature and % recovered liquid phase profile of PMMAW depolymerization at 450 °C.

3.2.2. Scaling-Up Effect in Chemical Composition of Liquid Phase

It can be analyzed the effect of increasing the production scale in the concentration of MMA in the liquid phase, displayed in graph of Figure 10, as functions of reaction time. The weighted average of MMA concentration in the liquid phase (considering the weight of each time-fractioned sample) is shown in the graph along the obtained MMA concentration of liquid bio-oil from laboratory scale, since the initial low feed weight made it impractical to divide laboratory bio-oil according to reaction time. The detailed chemical composition of all samples is supplied in Tables S1-S* as Supplementary Material.

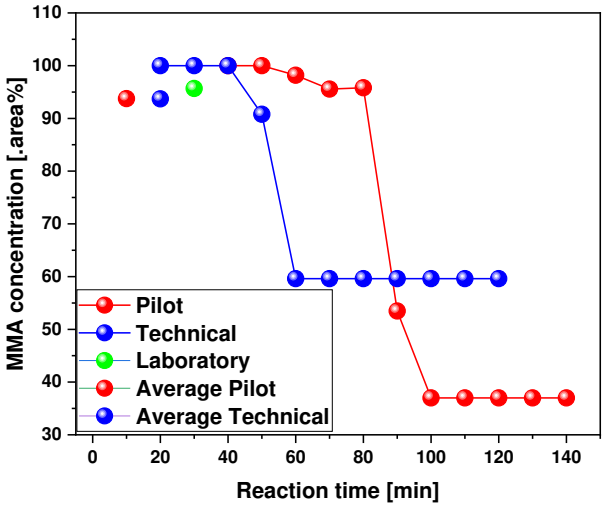

Figure 10. MMA concentration of liquid phase of the three different production scales.

Preprints (www.preprints.org) | NOT PEER-REVIEWED | Posted: 16 January 2024 doi:10.20944/preprints202401.1188.v1

Both curves of concentration of MMA in the technical and pilot plants show similar behavior with respect to reaction time, maintaining values near purity (>90 area.%) until a limiting moment is reached, of 40 and 80 minutes for the technical and pilot plants, respectively. In batch or semi-batch processes, the reaction time is directly proportional to the amount of feed present, and the process takes more time in the pilot reactor but maintaining some key aspects of the process. Comparing the graph of Figure 10 with the temperature profile of the pilot plant (Figure 7) shows that after 80 minutes, more than 90 % of the liquid phase was already collected in the separating drum in temperatures between 150-210 °C. It is interesting to note that, even though there was change in chemical composition of liquid fraction for all process scales (as it should on a semi-batch process), average composition changed little between all process scales, slightly increasing for the laboratory (95.7%) when compared with technical and pilot scales (93.7%), revealing that reaction mechanism is not affected by the increase in process scale even if liquid yields are fairly different, as shown in Table 3, suggesting even further that a temperature gradient across the fixed bed (provoked by the increase in process scale) is responsible by the differences in product yields. As the reaction proceeds, the polymeric chain unzips, forming MMA until condensation of products into polycyclic aromatic hydrocarbons and subsequently, char, occurring in higher temperatures [64]. With higher heating rates, the unzipping reaction of the polymer occur until little to no char is formed, while in the case of larger fixed beds of feed, the outer part of the reactor reaches high temperatures and the lower heating rates allows the formation of more char and gases, produced by the cracking of formed coal, producing aromatic hydrocarbons [81].

The formation of side products in the liquid fraction of PMMAW depolymerization process is limited to a few substances, like methyl isobutyrate and aromatic hydrocarbons as toluene, xylene, mesytilene and naphthalene. These aromatic compounds are formed in practically every pyrolysis, being part of the mechanism of char formation [82], as it was explained before. Methyl isobutyrate is formed probably by hydrogenation of MMA, during char formation, hydrogen is released and could be used for the hydrogenation of MMA to methyl isobutyrate. Figure 11 presents the variation of chemical composition of minor compounds present in the liquid fraction of technical scale. A similar behavior was observed in the pilot scale reactor and its chemical composition is presented in Figure 12.

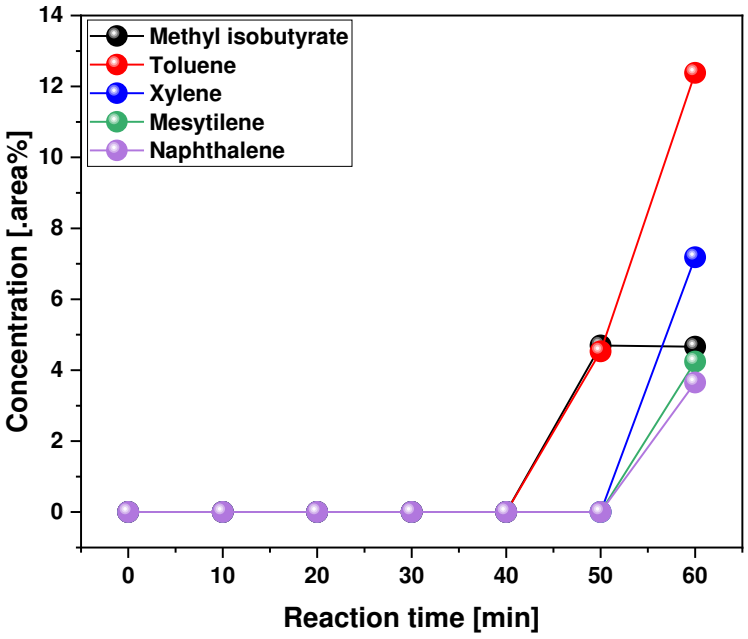

Preprints (www.preprints.org) | NOT PEER-REVIEWED | Posted: 16 January 2024 doi:10.20944/preprints202401.1188.v1

Figure 11. Concentration of side-products of liquid fraction of PMMAW depolymerization in technical scale.

It is possible to visualize the same trend in both production scales, with liquid fraction composition mainly formed by MMA and later in the process changes to a more varied chemical composition reminiscent of the polymer chain cracking, with compounds as methyl isobutyrate and EGDMA, as well as aromatic hydrocarbons produced by the cracking of char formed in the later stages of the pyrolysis process. The larger scale (pilot) also produced a non-identified heavy fraction, and it is not clear why it is not present in the liquid fraction formed in the technical scale. Due to the increased volume and mass flow in the pilot scale, the process takes longer and fractioning liquid samples according to reaction time produces a more detailed version of the chemical composition variation of the samples as the feed changes. For the lower mass of the technical scale, fractioning of samples each 10 minutes is not sufficient to obtain a detailed chemical composition and some compounds could not be adequately detected such as EGDMA and other aromatic hydrocarbons, detected in the pilot scale GC-MS spectra collected. The same could be said for the non-identified fraction: in the technical scale GC-MS they are probably present but could not be detected because they are present only in very small quantities, not showing appreciable concentration for detection in GC-MS. This is corroborated by the low mass fraction of the samples where it showed presence of NIC's (90 and 100 minutes of reaction time), of 6 and 2% of the recovered liquid, respectively.

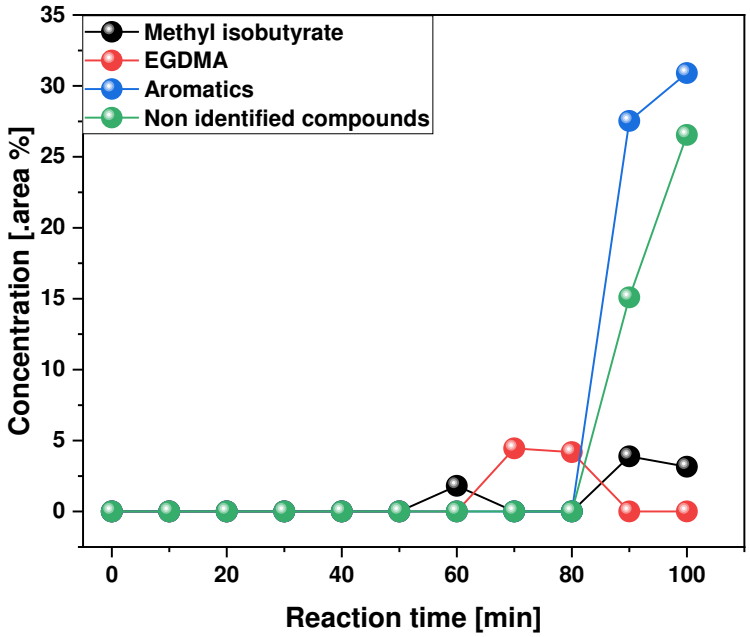

Figure 12. Concentration of side-products of liquid fraction of PMMAW depolymerization in pilot scale.

The chemical composition variation of the liquid fraction of PMMAW depolymerization is further analyzed by conducting experiments in technical scale in different temperatures (Figure 13). For the experiments conducted using 425 °C as setpoint temperature allowed for obtaining a liquid fraction almost exclusively composed of MMA, whereas for higher temperatures, MMA concentration tends to reduce with increasing setpoint temperature. As it was explained earlier, in a semi-batch pyrolysis process the reactor setpoint largely controls the extent of the reaction and only a small difference separates one experiment to the other. It is important to remember that even with decaying MMA concentration, on average the liquid fraction obtained during depolymerization presents high MMA concentration (higher than 90%) for all temperatures. Different heating rates and

Preprints (www.preprints.org) | NOT PEER-REVIEWED | Posted: 16 January 2024 doi:10.20944/preprints202401.1188.v1

different temperature gradients are observed though, especially for larger sized reactors, as the technical and pilot reactors, obtaining different product yields. For temperatures of 425 °C as setpoint, this temperature gradient is minimized obtaining a purified product and a higher amount of liquid. Reaction conducted at 425°C obtained liquid fraction yield of 81% against 61.7% and 61.3% for 450 and 475°C, respectively, showing the effect of minimization of this temperature gradient across the fixed heated zone of the reactor. Homogeneous temperature distribution is key in producing a liquid fraction with high yield and chemical composition of MMA.

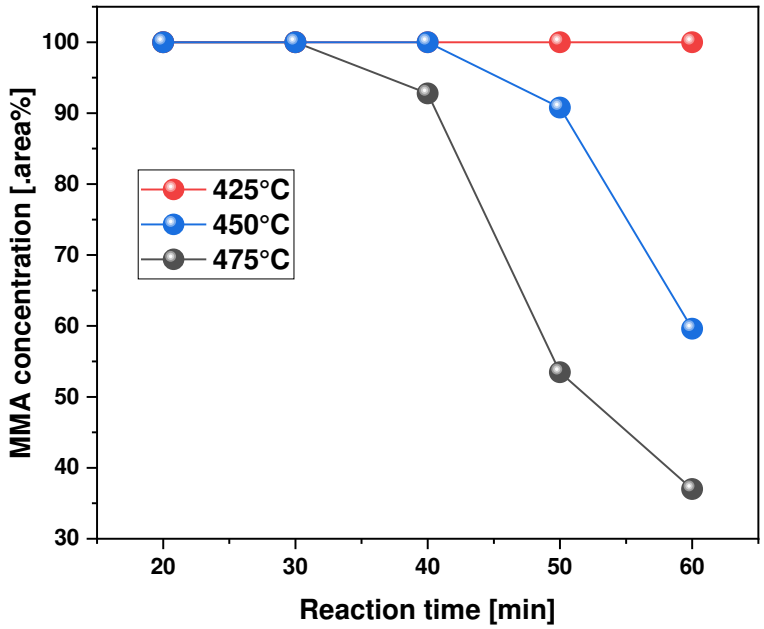

Figure 13. MMA Concentration of liquid fraction of PMMAW depolymerization in technical scale.

4. Discussion

In a previous work we detailed PMMA depolymerization process from a temperature perspective influence in pilot scale [9]. Now, based on the differences found in smaller scales, we presented detailed aspects of the three production scales of PMMAW depolymerization and highlight directions and choices in process design of PMMA depolymerization in fixed-bed semi batch reactors. These types of reactors are among the simplest and cheaper choices, offering great opportunity in the case of PMMA recycling process because depolymerization achieve liquid yields higher than 80% with MMA concentration of 90% [10–12,14,38,52]. As feedstock, we used waste PMMA from dental material.

First, the waste is characterized in micro-scale, by TG and DSC analysis and the thermal degradation curves (weight loss and DTG) are related to the possible mechanism of thermal degradation of PMMA. At low temperatures (200-300 °C), the reaction is initiated in the chain-end and depropagated to the rest of the chain via a radical mechanism causing an unzipping of the polymer chain until termination by a bimolecular interaction. At higher temperatures (400-500 °C), the mechanism changes to a random scission-initiated mechanism [64]. Even though it is possible to fit kinetic parameters considering more stages of decomposition [20,47], a single step mechanism is capable of accurately describe thermal decomposition of PMMAW, simplifying calculations and process design.

The heat flow involved in PMMAW decomposition was measured by DSC and presents important parameters for pyrolysis processes design such as the heat of gasification, the amount of energy required to heat, depolymerize and vaporize the products of pyrolysis and could mean the

 doi:10.20944/preprints202401.1188.v1

approval or rejection of certain designs based on the economics of MMA recovery process. Integration of DSC curve produced values of -423 J/g for the decomposition peak and -1740 J/g for heat of gasification. Even though it is an established tool for analysis of chemical reactions of solid samples such as glass transition temperatures and calculation of heat of reactions, DSC has to be standardized for analysis of pyrolysis processes due to some specifics. The technique presents great potential for the energetic analysis and process design of potential recycling processes by pyrolysis. Much of the variation in DSC analysis in pyrolysis processes arise from the following facts: there is weight change of the sample during pyrolysis and variation of its heat capacity as volatiles flow out of the furnace and char is formed; a detailed mechanism of degradation must be known to accurately identify and measure heats of reaction of individual peaks; there are many ways to extract the heat capacity variation from the DSC curve as linear regression, fitting functions and others [68,78]. The heat of gasification measured (since it is based on an integral value) presents similarities with others in academic literature [78–80], while the peak of decomposition energy (-423 J/g) seems to only represent a part of the actual heat of decomposition of PMMAW, which should be at least represented by the sum of heat of depolymerization (-578 J/g) and vaporization enthalpy of MMA (401 J/g) . Nevertheless, DSC revealed to be an important tool in investigation of the energy involved in pyrolysis processes and we certainly will refine and use it for upcoming research since energy balances are rarely considered in process design papers.

The three production scales were analyzed from a material balance perspective by reaction products yields and MMA concentration of the liquid phase, concluding that there is a temperature gradient across the fixed bed of PMMAW in the semi-batch reactors that negatively influence both liquid yield and MMA concentration. This gradient seems to be larger in the case of thick beds such as the technical and pilot scales. We defined two variables called reactor load and power load, related to the weight of feed to the available volume of the reactor and the available power to the weight of feed, respectively. The results shown that between the three process scales, both reactor and power loads decreased with increase in process scale and the result is decreased temperature of pyrolysis (200-300 °C) in the case of technical and pilot scales, while the laboratory scale produced results similar to the ones produced in micro-scale (TG), with degradation in higher temperatures such as 300-450 °C. In fact, due to positioning of the thermocouple (center of the fixed bed) controlling the reaction, much higher temperatures were probably involved in the rims, causing decrease in liquid yields and augmenting gas production. This is corroborated by the influence of temperature in the MMA concentration in liquid fraction, where it is shown that increased temperature reduces MMA concentration, observed in the experiments conducted in technical and pilot scales.

It is shown that, for most of the reaction time, liquid fraction is formed almost exclusively of MMA and in the final stages convert to liquid rich in aromatic hydrocarbons, suggesting that they are products of the remaining char that is being formed and simultaneously pyrolyzed. Even though little to no char is formed for smaller beds, there is a tendency to char increase with process scale due to increase in bed thickness and slower effective heating rate across the fixed bed, increasing char yields.

Finally, it is observed that lower temperatures (inferior to 450 °C) seem to produce liquid fractions formed almost exclusively of MMA, even with temperature gradient across the reactor, showing that lower temperatures and heating rates are beneficial to PMMA depolymerization in semi-batch mode. These findings represent a new way of analyzing a pyrolysis process due to focus in reactor design and economics calculation, extremely important in the case of viability of recycling processes. Upcoming works should improve on the ideas detailed in this paper, slowly establishing a standard protocol of analysis and design of pyrolysis and other processes.

Supplementary Materials: The following supporting information can be downloaded at: www.mdpi.com/xxx/s1. Table S1. Class of compounds, sum of peak areas, chemistry registry numbers (CAS), and retention times of molecules identified by gas chromatography-mass spectrometry (GC-MS) in the liquid phase by depolymerization of PMMA based dental resins fragments/residues at 425 °C, atmospheric pressure, and reaction times of 20, 30, 40, 50, and 60 minutes, in technical scale. Table S2. Class of compounds, sum of peak areas, chemistry registry numbers (CAS), and retention times of molecules identified by gas chromatography-mass spectrometry (GC-MS) in the liquid phase by depolymerization of PMMA based dental resins

fragments/residues at 450 °C, atmospheric pressure, and reaction times of 30, 40, 50, and 60 minutes, in technical scale. Table S3. Class of compounds, sum of peak areas, chemistry registry numbers (CAS), and retention times of molecules identified by gas chromatography-mass spectrometry (GC-MS) in the liquid phase by depolymerization of PMMA based dental resins fragments/residues at 475 °C, atmospheric pressure, and reaction times of 20, 30, 40, 50, and 60 minutes, in technical scale. Table S4. Class of compounds, sum of peak areas, chemistry registry numbers (CAS), and retention times of molecules identified by gas chromatography-mass spectrometry (GC-MS) in the liquid phase by depolymerization of PMMA based dental resins fragments/residues at 450 °C, atmospheric pressure, and reaction times of 40, 50, 60, 70, 80, 90, and 100 minutes, in pilot scale.

Author Contributions: The individual contributions of all the co-authors are provided as follows: (H.J.d.S.R.) contributed with formal analysis and writing original draft preparation, investigation and methodology, (A.C.R.) contributed with investigation and methodology, (C.C.F.) contributed with investigation and methodology, (L.M.P.) contributed with investigation and methodology, (M.C.S.) contributed with investigation and methodology, (L.H.H.G.) contributed with investigation and methodology, (F.P.d.C.A.) contributed with investigation and methodology, (S.A.P.d.M.) contributed with investigation and methodology, (D.A.R.d.C.) contributed with investigation and methodology, (S.D.J.) contributed with resources, chemical analysis, (L.E.P.B.) with investigation, methodology, and resources, (N.T.M.) contributed with supervision, conceptualization, and data curation, and (L.P.B.) contributed with co-supervision,. All authors have read and agreed to the published version of the manuscript.

Funding: This research received no external funding.

Institutional Review Board Statement: Not applicable.

Informed Consent Statement: Not applicable.

Acknowledgments: I would like to acknowledge and dedicate this research in memory to Hélio da Silva Almeida, Professor at the Faculty of Sanitary and Environmental Engineer-ing/UFPa, who passed away on 13 March 2021. His contagious joy, dedication, intelligence, honesty, seriousness, and kindness will always be remembered in our hearts.

Conflicts of Interest: The authors declare no conflict of interest.

References

1. Dai, L.; Zhou, N.; Lv, Y.; Cheng, Y.; Wang, Y.; Liu, Y.; Cobb, K.; Chen, P.; Lei, H.; Ruan, R. Pyrolysis Technology for Plastic Waste Recycling: A State-of-the-Art Review. *Prog Energy Combust Sci* **2022**, *93*, 101021, doi:10.1016/j.pecs.2022.101021.
2. Ali, U.; Karim, K.J.B.A.; Buang, N.A. A Review of the Properties and Applications of Poly (Methyl Methacrylate) (PMMA). *Polymer Reviews* **2015**, *55*, 678–705, doi:10.1080/15583724.2015.1031377.
3. Frazer, R.Q.; Byron, R.T.; Osborne, P.B.; West, K.P. PMMA: An Essential Material in Medicine and Dentistry. *J Long Term Eff Med Implants* **2005**, *15*, 629–639, doi:10.1615/JLONGTERMEFFMEDIMPLANTS.V15.I6.60.
4. Gozum, N.; Safgonul Unal, E.; Altan-Yaycioglu, R.; Gucukoglu, A.; Ozgun, C. Visual Performance of Acrylic and PMMA Intraocular Lenses. *Eye (Lond)* **2003**, *17*, 238–242, doi:10.1038/SJ.EYE.6700290.
5. Spasojevic, P.; Zrilic, M.; Panic, V.; Stamenkovic, D.; Seslija, S.; Velickovic, S. The Mechanical Properties of a Poly(Methyl Methacrylate) Denture Base Material Modified with Dimethyl Itaconate and Di-n-Butyl Itaconate. *Int J Polym Sci* **2015**, *2015*, doi:10.1155/2015/561012.
6. Gigault, J.; Halle, A. ter; Baudrimont, M.; Pascal, P.Y.; Gauffre, F.; Phi, T.L.; El Hadri, H.; Grassl, B.; Reynaud, S. Current Opinion: What Is a Nanoplastic? *Environmental Pollution* **2018**, *235*, 1030–1034, doi:10.1016/J.ENVPOL.2018.01.024.
7. Rillig, M.C.; Lehmann, A. Microplastic in Terrestrial Ecosystems. *Science (1979)* **2020**, *368*, 1430–1431, doi:10.1126/SCIENCE.ABB5979.
8. Fatih Demirbas, M. Biorefineries for Biofuel Upgrading: A Critical Review. *Appl Energy* **2009**, *86*, S151–S161, doi:10.1016/j.apenergy.2009.04.043.
9. Dos Santos, P.B.; da Silva Ribeiro, H.J.; Ferreira, A.C.; Ferreira, C.C.; Bernar, L.P.; da Costa Assunção, F.P.; de Castro, D.A.R.; Santos, M.C.; Duvoisin, S.; Borges, L.E.P.; et al. Process Analysis of PMMA-Based Dental Resins Residues Depolymerization: Optimization of Reaction Time and Temperature. *Energies 2022, Vol. 15, Page 91* **2021**, *15*, 91, doi:10.3390/EN15010091.
10. Kaminsky, W.; Predel, M.; Sadiki, A. Feedstock Recycling of Polymers by Pyrolysis in a Fluidised Bed. *Polym Degrad Stab* **2004**, *85*, 1045–1050, doi:10.1016/J.POLYMDEGRADSTAB.2003.05.002.

11. Kaminsky, W.; Franck, J. Monomer Recovery by Pyrolysis of Poly(Methyl Methacrylate) (PMMA). *J Anal Appl Pyrolysis* **1991**, *19*, 311–318, doi:10.1016/0165-2370(91)80052-A.
12. KAMINSKY, W. Recycling of Polymers by Pyrolysis. *Le Journal de Physique IV* **1993**, *03*, C7-1543-C7-1552, doi:10.1051/jp4:19937241.
13. Arisawa, H.; Brill, T.B. Kinetics and Mechanisms of Flash Pyrolysis of Poly(Methyl Methacrylate) (PMMA). *Combust Flame* **1997**, *109*, 415–426, doi:10.1016/S0010-2180(96)00190-3.
14. Kaminsky, W.; Eger, C. Pyrolysis of Filled PMMA for Monomer Recovery. *J Anal Appl Pyrolysis* **2001**, *58–59*, 781–787, doi:10.1016/S0165-2370(00)00171-6.
15. Smolders, K.; Baeyens, J. Thermal Degradation of PMMA in Fluidised Beds. *Waste Manag* **2004**, *24*, 849–857, doi:10.1016/J.WASMAN.2004.06.002.
16. Kang, B.S.; Kim, S.G.; Kim, J.S. Thermal Degradation of Poly(Methyl Methacrylate) Polymers: Kinetics and Recovery of Monomers Using a Fluidized Bed Reactor. *J Anal Appl Pyrolysis* **2008**, *81*, 7–13, doi:10.1016/J.JAAP.2007.07.001.
17. Achilias, D.S. Chemical Recycling of Poly(Methyl Methacrylate) by Pyrolysis. Potential Use of the Liquid Fraction as a Raw Material for the Reproduction of the Polymer. *Eur Polym J* **2007**, *43*, 2564–2575, doi:10.1016/J.EURPOLYMJ.2007.02.044.
18. Lopez, G.; Artetxe, M.; Amutio, M.; Elordi, G.; Aguado, R.; Olazar, M.; Bilbao, J. Recycling Poly-(Methyl Methacrylate) by Pyrolysis in a Conical Spouted Bed Reactor. *Chemical Engineering and Processing: Process Intensification* **2010**, *49*, 1089–1094, doi:10.1016/J.CEP.2010.08.002.
19. Szabo, E.; Olah, M.; Ronkay, F.; Miskolczi, N.; Blazso, M. Characterization of the Liquid Product Recovered through Pyrolysis of PMMA–ABS Waste. *J Anal Appl Pyrolysis* **2011**, *92*, 19–24, doi:10.1016/J.JAAP.2011.04.008.
20. Braido, R.S.; Borges, L.E.P.; Pinto, J.C. Chemical Recycling of Crosslinked Poly(Methyl Methacrylate) and Characterization of Polymers Produced with the Recycled Monomer. *J Anal Appl Pyrolysis* **2018**, *132*, 47–55, doi:10.1016/J.JAAP.2018.03.017.
21. Zeng, W.R.; Li, S.F.; Chow, W.K. Review on Chemical Reactions of Burning Poly(Methyl Methacrylate) PMMA. *http://dx.doi.org/10.1177/0734904102020005482* **2002**, *20*, 401–433, doi:10.1177/0734904102020005482.
22. Hirata, T.; Kashiwagi, T.; Brown, J.E. Thermal and Oxidative Degradation of Poly(Methyl Methacrylate): Weight Loss. *Macromolecules* **1985**, *18*, 1410–1418.
23. Manring, L.E. Thermal Degradation of Poly(Methyl Methacrylate). 2. Vinyl-Terminated Polymer. *A. Rev. Plast. Mod* **1969**, *19*, 1515.
24. Peterson, J.D.; Vyazovkin, S.; Wight, C.A. Kinetic Study of Stabilizing Effect of Oxygen on Thermal Degradation of Poly(Methyl Methacrylate). *Journal of Physical Chemistry B* **1999**, *103*, 8087–8092, doi:10.1021/JP991582D/ASSET/IMAGES/LARGE/JP991582DF2.JPEG.
25. Hu, Y.H.; Chen, C.Y. The Effect of End Groups on the Thermal Degradation of Poly(Methyl Methacrylate). *Polym Degrad Stab* **2003**, *82*, 81–88, doi:10.1016/S0141-3910(03)00165-4.
26. Ferriol, M.; Gentilhomme, A.; Cochez, M.; Oget, N.; Mieloszynski, J.L. Thermal Degradation of Poly(Methyl Methacrylate) (PMMA): Modelling of DTG and TG Curves. *Polym Degrad Stab* **2003**, *79*, 271–281, doi:10.1016/S0141-3910(02)00291-4.
27. Gao, Z.; Kaneko, T.; Hou, D.; Nakada, M. Kinetics of Thermal Degradation of Poly(Methyl Methacrylate) Studied with the Assistance of the Fractional Conversion at the Maximum Reaction Rate. *Polym Degrad Stab* **2004**, *84*, 399–403, doi:10.1016/J.POLYMDEGRADSTAB.2003.11.015.
28. Motaung, T.E.; Luyt, A.S.; Bondioli, F.; Messori, M.; Saladino, M.L.; Spinella, A.; Nasillo, G.; Caponetti, E. PMMA–Titania Nanocomposites: Properties and Thermal Degradation Behaviour. *Polym Degrad Stab* **2012**, *97*, 1325–1333, doi:10.1016/J.POLYMDEGRADSTAB.2012.05.022.
29. Fateh, T.; Richard, F.; Rogaume, T.; Joseph, P. Experimental and Modelling Studies on the Kinetics and Mechanisms of Thermal Degradation of Polymethyl Methacrylate in Nitrogen and Air. *J Anal Appl Pyrolysis* **2016**, *120*, 423–433, doi:10.1016/J.JAAP.2016.06.014.
30. Bhargava, A.; Van Hees, P.; Andersson, B. Pyrolysis Modeling of PVC and PMMA Using a Distributed Reactivity Model. *Polym Degrad Stab* **2016**, *129*, 199–211, doi:10.1016/J.POLYMDEGRADSTAB.2016.04.016.
31. Cheng, J.; Pan, Y.; Yao, J.; Wang, X.; Pan, F.; Jiang, J. Mechanisms and Kinetics Studies on the Thermal Decomposition of Micron Poly (Methyl Methacrylate) and Polystyrene. *J Loss Prev Process Ind* **2016**, *40*, 139–146, doi:10.1016/J.JLP.2015.12.017.
32. Holland, B.J.; Hay, J.N. The Kinetics and Mechanisms of the Thermal Degradation of Poly(Methyl Methacrylate) Studied by Thermal Analysis-Fourier Transform Infrared Spectroscopy. *Polymer (Guildf)* **2001**, *42*, 4825–4835, doi:10.1016/S0032-3861(00)00923-X.

33. Ozlem, S.; Aslan-Gürel, E.; Rossi, R.M.; Hacaloglu, J. Thermal Degradation of Poly(Isobornyl Acrylate) and Its Copolymer with Poly(Methyl Methacrylate) via Pyrolysis Mass Spectrometry. *J Anal Appl Pyrolysis* **2013**, *100*, 17–25, doi:10.1016/J.JAAP.2012.10.024.
34. Özlem-Gundogdu, S.; Gurel, E.A.; Hacaloglu, J. Pyrolysis of of Poly(Methy Methacrylate) Copolymers. *J Anal Appl Pyrolysis* **2015**, *113*, 529–538, doi:10.1016/J.JAAP.2015.03.015.
35. Manring, L.E. Thermal Degradation of Poly(Methyl Methacrylate). 4. Random Side-Group Scissiont. *Macromolecules* **1991**, *24*, 3304–3309.
36. Godiya, C.B.; Gabrielli, S.; Materazzi, S.; Pianesi, M.S.; Stefanini, N.; Marcantoni, E. Depolymerization of Waste Poly(Methyl Methacrylate) Scraps and Purification of Depolymerized Products. *J Environ Manage* **2019**, *231*, 1012–1020, doi:10.1016/J.JENVMAN.2018.10.116.
37. Popescu, V.; Vasile, C.; Brebu, M.; Popescu, G.L.; Moldovan, M.; Prejmerean, C.; Stănuleţ, L.; Trişcă-Rusu, C.; Cojocaru, I. The Characterization of Recycled PMMA. *J Alloys Compd* **2009**, *483*, 432–436, doi:10.1016/J.JALLCOM.2008.08.148.
38. Grause, G.; Predel, M.; Kaminsky, W. Monomer Recovery from Aluminium Hydroxide High Filled Poly(Methyl Methacrylate) in a Fluidized Bed Reactor. *J Anal Appl Pyrolysis* **2006**, *75*, 236–239, doi:10.1016/J.JAAP.2005.06.006.
39. Newborough, M.; Highgate, D.; Vaughan, P. Thermal Depolymerisation of Scrap Polymers. *Appl Therm Eng* **2002**, *22*, 1875–1883, doi:10.1016/S1359-4311(02)00115-1.
40. Sasaki, A.; Tsuji, T. POLY(METHYL METHACRYLATE) PYROLYSIS BY TWO FLUIDIZED BED PROCESS.
41. Zeng, W.R.; Li, S.F.; Chow, W.K. Preliminary Studies on Burning Behavior of Polymethylmethacrylate (PMMA). *http://dx.doi.org/10.1177/073490402762574749* **2002**, *20*, 297–317, doi:10.1177/073490402762574749.
42. Chen, R.; Xu, M. Kinetic and Volatile Products Study of Micron-Sized PMMA Waste Pyrolysis Using Thermogravimetry and Fourier Transform Infrared Analysis. *Waste Management* **2020**, *113*, 51–61, doi:10.1016/J.WASMAN.2020.05.039.
43. Chen, R.; Li, Q.; Xu, X.; Zhang, D. Pyrolysis Kinetics and Reaction Mechanism of Representative Non-Charring Polymer Waste with Micron Particle Size. *Energy Convers Manag* **2019**, *198*, 111923, doi:10.1016/J.ENCONMAN.2019.111923.
44. Jayarama Krishna, J. V.; Srivatsa Kumar, S.; Korobeinichev, O.P.; Vinu, R. Detailed Kinetic Analysis of Slow and Fast Pyrolysis of Poly(Methyl Methacrylate)-Flame Retardant Mixtures. *Thermochim Acta* **2020**, *687*, 178545, doi:10.1016/J.TCA.2020.178545.
45. Özsin, G. Assessing Thermal Behaviours of Cellulose and Poly(Methyl Methacrylate) during Co-Pyrolysis Based on an Unified Thermoanalytical Study. *Bioresour Technol* **2020**, *300*, 122700, doi:10.1016/J.BIORTECH.2019.122700.
46. Korobeinichev, O.P.; Paletsky; Gonchikzhapov, M.B.; Glaznev, R.K.; Gerasimov, I.E.; Naganovsky, Y.K.; Shundrina, I.K.; Snegirev, A.Y.; Vinu, R. Kinetics of Thermal Decomposition of PMMA at Different Heating Rates and in a Wide Temperature Range. *Thermochim Acta* **2019**, *671*, 17–25, doi:10.1016/J.TCA.2018.10.019.
47. Da Ros, S.; Braido, R.S.; de Souza e Castro, N.L.; Brandão, A.L.T.; Schwaab, M.; Pinto, J.C. Modelling the Chemical Recycling of Crosslinked Poly (Methyl Methacrylate): Kinetics of Depolymerisation. *J Anal Appl Pyrolysis* **2019**, *144*, 104706, doi:10.1016/J.JAAP.2019.104706.
48. Poudel, J.; Lee, Y.M.; Kim, H.J.; Oh, S.C. Methyl Methacrylate (MMA) and Alumina Recovery from Waste Artificial Marble Powder Pyrolysis. *J Mater Cycles Waste Manag* **2021**, *23*, 214–221, doi:10.1007/S10163-020-01120-4/FIGURES/7.
49. Snegirev, A.Y.; Talalov, V.A.; Stepanov, V. V.; Korobeinichev, O.P.; Gerasimov, I.E.; Shmakov, A.G. Autocatalysis in Thermal Decomposition of Polymers. *Polym Degrad Stab* **2017**, *137*, 151–161, doi:10.1016/J.POLYMDEGRADSTAB.2017.01.008.
50. Handawy, M.K.; Snegirev, A.Y.; Stepanov, V. V; Talalov, V.A. Kinetic Modeling and Analysis of Pyrolysis of Polymethyl Methacrylate Using Isoconversional Methods. *IOP Conf Ser Mater Sci Eng* **2021**, *1100*, 012053, doi:10.1088/1757-899X/1100/1/012053.
51. Chen, R.; Pan, R.; Li, Q. Thermal Degradation Characteristics, Kinetics and Thermodynamics of Micron-Sized PMMA in Oxygenous Atmosphere Using Thermogravimetry and Deconvolution Method Based on Gauss Function. *J Loss Prev Process Ind* **2021**, *71*, 104488, doi:10.1016/J.JLP.2021.104488.
52. Kaminsky, W. Thermal Recycling of Polymers. *J Anal Appl Pyrolysis* **1985**, *8*, 439–448, doi:10.1016/0165-2370(85)80042-5.
53. Ding, Y.; Chen, W.; Zhang, W.; Zhang, X.; Li, C.; Zhou, R.; Miao, F. Experimental and Numerical Simulation Study of Typical Semi-Transparent Material Pyrolysis with in-Depth Radiation Based on Micro and Bench Scales. *Energy* **2022**, *258*, 124863, doi:10.1016/J.ENERGY.2022.124863.

54. Bate, D.M.; Lehrle, R.S. A New Approach for Measuring the Rate of Pyrolysis of Cross-Linked Polymers: Evaluation of Degradation Rate Constants for Cross-Linked PMMA. *Polym Degrad Stab* **1998**, *62*, 67–71, doi:10.1016/S0141-3910(97)00262-0.
55. de Freitas Costa, A.F.; Ferreira, C.C.; da Paz, S.P.A.; Santos, M.C.; Moreira, L.G.S.; Mendonça, N.M.; da Costa Assunção, F.P.; de Freitas, A.C.G. de A.; Costa, R.M.R.; de Sousa Brandão, I.W.; et al. Catalytic Upgrading of Plastic Waste of Electric and Electronic Equipment (WEEE) Pyrolysis Vapors over Si–Al Ash Pellets in a Two-Stage Reactor. *Energies (Basel)* **2023**, *16*, 541, doi:10.3390/en16010541.
56. Ferreira, C.C.; Bernar, L.P.; de Freitas Costa, A.F.; da Silva Ribeiro, H.J.; Santos, M.C.; Moraes, N.L.; Costa, Y.S.; Baia, A.C.F.; Mendonça, N.M.; da Mota, S.A.P.; et al. Improving Fuel Properties and Hydrocarbon Content from Residual Fat Pyrolysis Vapors over Activated Red Mud Pellets in Two-Stage Reactor: Optimization of Reaction Time and Catalyst Content. *Energies (Basel)* **2022**, *15*, 5595, doi:10.3390/en15155595.
57. Pinto Bernar, L.; Campos Ferreira, C.; Fernando de Freitas Costa, A.; Jorge da Silva Ribeiro, H.; Gomes dos Santos, W.; Martins Pereira, L.; Mathias Pereira, A.; Lobato Moraes, N.; Paula da Costa Assunção, F.; Alex Pereira da Mota, S.; et al. Catalytic Upgrading of Residual Fat Pyrolysis Vapors over Activated Carbon Pellets into Hydrocarbons-like Fuels in a Two-Stage Reactor: Analysis of Hydrocarbons Composition and Physical-Chemistry Properties. *Energies 2022, Vol. 15, Page 4587* **2022**, *15*, 4587, doi:10.3390/EN15134587.
58. da Mota, S.A.P.; Mancio, A.A.; Lhamas, D.E.L.; de Abreu, D.H.; da Silva, M.S.; dos Santos, W.G.; de Castro, D.A.R.; de Oliveira, R.M.; Araújo, M.E.; Borges, L.E.P.; et al. Production of Green Diesel by Thermal Catalytic Cracking of Crude Palm Oil (Elaeis Guineensis Jacq) in a Pilot Plant. *J Anal Appl Pyrolysis* **2014**, *110*, 1–11, doi:10.1016/j.jaap.2014.06.011.
59. Daniel Valdez, G.; Valois, F.; Bremer, S.; Bezerra, K.; Hamoy Guerreiro, L.; Santos, M.; Bernar, L.; Feio, W.; Moreira, L.; Mendonça, N.; et al. Improving the Bio-Oil Quality of Residual Biomass Pyrolysis by Chemical Activation: Effect of Alkalis and Acid Pre-Treatment. *Energies (Basel)* **2023**, *16*, 3162, doi:10.3390/en16073162.
60. Rocha de Castro, D.; da Silva Ribeiro, H.; Hamoy Guerreiro, L.; Pinto Bernar, L.; Jonatan Bremer, S.; Costa Santo, M.; da Silva Almeida, H.; Duvoisin, S.; Pizarro Borges, L.; Teixeira Machado, N. Production of Fuel-Like Fractions by Fractional Distillation of Bio-Oil from Açaí (Euterpe Oleracea Mart.) Seeds Pyrolysis. *Energies (Basel)* **2021**, *14*, 3713, doi:10.3390/en14133713.
61. da Silva Almeida, H.; Corrêa, O.A.; Eid, J.G.; Ribeiro, H.J.; de Castro, D.A.R.; Pereira, M.S.; Pereira, L.M.; de Andrade Mâncio, A.; Santos, M.C.; da Silva Souza, J.A.; et al. Production of Biofuels by Thermal Catalytic Cracking of Scum from Grease Traps in Pilot Scale. *J Anal Appl Pyrolysis* **2016**, *118*, 20–33, doi:10.1016/j.jaap.2015.12.019.
62. da Silva Almeida, H.; Corrêa, O.A.; Ferreira, C.C.; Ribeiro, H.J.; de Castro, D.A.R.; Pereira, M.S.; de Andrade Mâncio, A.; Santos, M.C.; da Mota, S.A.P.; da Silva Souza, J.A.; et al. Diesel-like Hydrocarbon Fuels by Catalytic Cracking of Fat, Oils, and Grease (FOG) from Grease Traps. *Journal of the Energy Institute* **2017**, *90*, 337–354, doi:10.1016/j.joei.2016.04.008.
63. Santos, M.C.; Lourenço, R.M.; de Abreu, D.H.; Pereira, A.M.; de Castro, D.A.R.; Pereira, M.S.; Almeida, H.S.; Mâncio, A.A.; Lhamas, D.E.L.; da Mota, S.A.P.; et al. Gasoline-like Hydrocarbons by Catalytic Cracking of Soap Phase Residue of Neutralization Process of Palm Oil (Elaeis Guineensis Jacq). *J Taiwan Inst Chem Eng* **2017**, *71*, 106–119, doi:10.1016/j.jtice.2016.11.016.
64. Barlow, A.; Lehrle, R.S.; Robb, J.C.; Sunderland, D. Polymethylmethacrylate Degradation—Kinetics and Mechanisms in the Temperature Range 340° to 460°C. *Polymer (Guildf)* **1967**, *8*, 537–545, doi:10.1016/0032-3861(67)90065-1.
65. Kumar, M.; Arun, S.; Upadhyaya, P.; Pugazhenthi, G. Properties of PMMA/Clay Nanocomposites Prepared Using Various Compatibilizers. *International Journal of Mechanical and Materials Engineering* **2015**, *10*, 7, doi:10.1186/s40712-015-0035-x.
66. Chen, Q.; Yang, R.; Zhao, B.; Li, Y.; Wang, S.; Wu, H.; Zhuo, Y.; Chen, C. Investigation of Heat of Biomass Pyrolysis and Secondary Reactions by Simultaneous Thermogravimetry and Differential Scanning Calorimetry. *Fuel* **2014**, *134*, 467–476, doi:10.1016/j.fuel.2014.05.092.
67. Ghanbari, E.; Picken, S.J.; van Esch, J.H. Analysis of Differential Scanning Calorimetry (DSC): Determining the Transition Temperatures, and Enthalpy and Heat Capacity Changes in Multicomponent Systems by Analytical Model Fitting. *J Therm Anal Calorim* **2023**, *148*, 12393–12409, doi:10.1007/s10973-023-12356-1.
68. Haseli, Y.; van Oijen, J.A.; de Goey, L.P.H. Modeling Biomass Particle Pyrolysis with Temperature-Dependent Heat of Reactions. *J Anal Appl Pyrolysis* **2011**, *90*, 140–154, doi:10.1016/j.jaap.2010.11.006.
69. Karlou, K.; Schneider, H.A. DSC and P-V-T Study of PVC/PMMA Blends. *J Therm Anal Calorim* **2000**, *59*, 59–69, doi:10.1023/A:1010119525345.
70. Poomalai, P.; Varghese, T.O. Thermomechanical Behaviour of Poly(Methyl Methacrylate)/Copoly(Ether-Ester) Blends. *ISRN Materials Science* **2011**, *2011*, 1–5, doi:10.5402/2011/921293.

71. Saxena, P.; Shukla, P.; Gaur, M. Thermal Analysis of Polymer Blends and Double Layer by DSC. *Polymers and Polymer Composites* **2021**, *29*, S11–S18, doi:10.1177/0967391120984606.
72. Hajduk, B.; Bednarski, H.; Jarka, P.; Janeczek, H.; Godzierz, M.; Tański, T. Thermal and Optical Properties of PMMA Films Reinforced with Nb2O5 Nanoparticles. *Sci Rep* **2021**, *11*, 22531, doi:10.1038/s41598-021-01282-7.
73. Wu, W.; Ouyang, Q.; He, L.; Huang, Q. Optical and Thermal Properties of Polymethyl Methacrylate (PMMA) Bearing Phenyl and Adamantyl Substituents. *Colloids Surf A Physicochem Eng Asp* **2022**, *653*, 130018, doi:10.1016/j.colsurfa.2022.130018.
74. Li, Y.; Guo, H. Crosslinked Poly(Methyl Methacrylate) with Perfluorocyclobutyl Aryl Ether Moiety as Crosslinking Unit: Thermally Stable Polymer with High Glass Transition Temperature. *RSC Adv* **2020**, *10*, 1981–1988, doi:10.1039/C9RA10166G.
75. Yin, W.; Xie, Z.; Yin, Y.; Yi, J.; Liu, X.; Wu, H.; Wang, S.; Xie, Y.; Yang, Y. Aging Behavior and Lifetime Prediction of PMMA under Tensile Stress and Liquid Scintillator Conditions. *Advanced Industrial and Engineering Polymer Research* **2019**, *2*, 82–87, doi:10.1016/j.aiepr.2019.04.002.
76. Chat, K.; Tu, W.; Beena Unni, A.; Adrjanowicz, K. Influence of Tacticity on the Glass-Transition Dynamics of Poly(Methyl Methacrylate) (PMMA) under Elevated Pressure and Geometrical Nanoconfinement. *Macromolecules* **2021**, *54*, 8526–8537, doi:10.1021/acs.macromol.1c01341.
77. Andreozzi, L.; Faetti, M.; Giordano, M.; Palazzuoli, D. Enthalpy Recovery in Low Molecular Weight PMMA. *J Non Cryst Solids* **2003**, *332*, 229–241, doi:10.1016/j.jnoncrysol.2003.09.006.
78. Fiola, G.J.; Chaudhari, D.M.; Stoliarov, S.I. Comparison of Pyrolysis Properties of Extruded and Cast Poly(Methyl Methacrylate). *Fire Saf J* **2021**, *120*, 103083, doi:10.1016/j.firesaf.2020.103083.
79. Alonso, A.; Lázaro, D.; Lázaro, M.; Alvear, D. Self-Heating Evaluation on Thermal Analysis of Polymethyl Methacrylate (PMMA) and Linear Low-Density Polyethylene (LLDPE). *J Therm Anal Calorim* **2022**, *147*, 10067–10081, doi:10.1007/S10973-022-11364-X/TABLES/6.
80. Wang, W.-H.; Su, W.; Hu, S.-Y.; Huang, Y.; Pan, Y.; Chang, S.-C.; Shu, C.-M. Pyrolysis Characteristics and Kinetics of Polymethylmethacrylate-Based Polymer Electrolytes for Lithium-Ion Battery. *J Therm Anal Calorim* **2022**, *147*, 12019–12032, doi:10.1007/s10973-022-11386-5.
81. Ren, X.-Y.; Feng, X.-B.; Cao, J.-P.; Tang, W.; Wang, Z.-H.; Yang, Z.; Zhao, J.-P.; Zhang, L.-Y.; Wang, Y.-J.; Zhao, X.-Y. Catalytic Conversion of Coal and Biomass Volatiles: A Review. *Energy & Fuels* **2020**, *34*, 10307–10363, doi:10.1021/acs.energyfuels.0c01432.

Chang, C.-Chu.; Wan, S.-Wu. China's Motor Fuels from Tung Oil. *Ind Eng Chem* **1947**, *39*, 1543–1548, doi:10.1021/ie50456a011.